

Geometric Properties of Central Catadioptric Line Images

João P. Barreto and Helder Araujo

Institute of Systems and Robotics
Dept. of Electrical and Computer Engineering
University of Coimbra
Coimbra, Portugal
{jpbar, helder}@isr.uc.pt
<http://www.isr.uc.pt/~jpbar>

Abstract. It is highly desirable that an imaging system has a single effective viewpoint. Central catadioptric systems are imaging systems that use mirrors to enhance the field of view while keeping a unique center of projection. A general model for central catadioptric image formation has already been established. The present paper exploits this model to study the catadioptric projection of lines. The equations and geometric properties of general catadioptric line imaging are derived. We show that it is possible to determine the position of both the effective viewpoint and the absolute conic in the catadioptric image plane from the images of three lines. It is also proved that it is possible to identify the type of catadioptric system and the position of the line at infinity without further information. A methodology for central catadioptric system calibration is proposed. Reconstruction aspects are discussed. Experimental results are presented. All the results presented are original and completely new.

1 Introduction

Many applications in computer vision, such as surveillance and model acquisition for virtual reality, require that a large field of view is imaged. Visual control of motion can also benefit from enhanced fields of view [1,2,4]. One effective way to enhance the field of view of a camera is to use mirrors [5,6,7,8,9]. The general approach of combining mirrors with conventional imaging systems is referred to as catadioptric image formation [3].

The fixed viewpoint constraint is a requirement ensuring that the visual sensor only measures the intensity of light passing through a single point in 3D space (the projection center). Vision systems verifying the fixed viewpoint constraint are called central projection systems. Central projection systems present interesting geometric properties. A single effective viewpoint is a necessary condition for the generation of geometrically correct perspective images [10], and for the existence of epipolar geometry inherent to the moving sensor and independent of the scene structure [1]. It is highly desirable for any vision system to have a single viewpoint. In [10], Baker et al. derive the entire class of catadioptric systems with a single effective viewpoint. Systems built using a parabolic

mirror with an orthographic camera, or an hyperbolic, elliptical or planar mirror with a perspective camera verify the fixed viewpoint constraint.

In [12], Geyer et al. introduce an unifying theory for all central catadioptric systems where conventional perspective imaging appears as a particular case. They show that central panoramic projection is isomorphic to a projective mapping from the sphere to a plane with a projection center on the perpendicular to the plane. A modified version of this unifying model is presented in [21]. The mapping between points in the 3D world and points in the catadioptric image plane is split into three steps. World points are mapped into an oriented projective plane by a linear function described by a 3×4 matrix (similar to the projective camera model referred in [13]). The oriented projective plane is then transformed by a non-linear function $f(\cdot)$. The last step is a collineation in the plane depending on the mirror parameters, the pose of the camera in relation to the reflective surface and the camera intrinsic parameters. The model obtained is general, intuitive and isolates the non-linear characteristics of general catadioptric image formation.

A line in 3D projects into a conic in a general catadioptric image. The equations and geometric properties of the resulting conic are derived in [12]. In [12,14] the intrinsic calibration of central catadioptric systems using line projections is discussed. A method to calibrate a system consisting of a paraboloid and an orthographic lens using two sets of parallel lines is presented in [14]. Our work uses the established mapping model to derive the equations and geometric properties of general central catadioptric line projections. The derived geometric properties are used to determine the position of the effective viewpoint and the absolute conic in the catadioptric plane from three line images. With the effective viewpoint and the absolute conic it is possible to compute the position of the line at infinity from two line images. Moreover we show that mirror parameters can be partially recovered directly from a single line image. The proposed theory is useful to both calibration and 3D reconstruction applications. Some experimental results are presented.

2 General Model for Central Catadioptric Imaging

In [10], Baker et al. derive the entire class of catadioptric systems with a single effective viewpoint. Systems built using a a parabolic mirror with an orthographic camera, or an hyperbolic, elliptical or planar mirror with a perspective camera verify the fixed viewpoint constraint. An unifying model for all central projection panoramic imaging is proposed in [12]. This section presents a modified version of this model.

Fig.1 is a scheme of the catadioptric system combining an hyperbolic reflective surface with a perspective camera. The hyperbola is placed such that its axis is the z -axis, its foci are coincident with O and O_{cam} (the origin of coordinate systems \mathcal{R} and \mathcal{R}_{cam}), its latus rectum is $4p$ and the distance between the foci is d . Light rays incident with O (the inner focal point) are reflected into rays incident with O_{cam} (the outer focal point). Assume a perspective camera with projection center in O_{cam} pointed to the mirror surface. All the captured light rays go originally through the inner focus of the hyperbolic surface. The effective viewpoint of the grabbed image is O and is unique. Elliptical catadioptric images are obtained combining an elliptical mirror with a perspective camera in a similar way. In the parabolic situation a parabolic mirror is

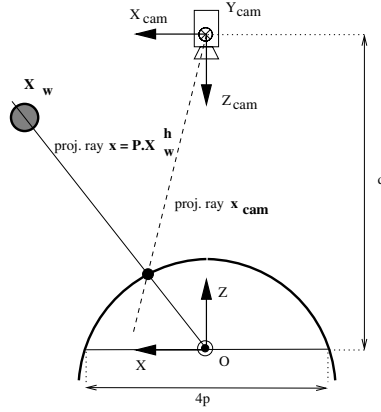


Fig. 1. Central catadioptric vision system

placed such that its axis is the z -axis, and its unique finite real focus is coincident with O . Light rays incident with O are reflected into rays parallel with the z -axis which are captured by an orthographic camera with image plane perpendicular to the z -axis. The effective viewpoint is in O and is unique. A catadioptric system made up of a perspective camera steering a planar mirror also verifies the fixed viewpoint constraint. The effective projection center is behind the mirror in the perpendicular line passing through camera center. Its distance to the camera center is twice the distance between the planar mirror and the camera.

Consider a generic scene point, visible by the catadioptric system, with cartesian coordinates \mathbf{X}_w in the catadioptric reference frame. The corresponding homogeneous representation is \mathbf{X}_w^h . Visible points in the scene \mathbf{X}_w^h are mapped into projective rays/points \mathbf{x} in the catadioptric system reference frame centered in the effective viewpoint. The transformation is linear being described by a 3×4 matrix \mathbf{P} . We can think of the projective rays \mathbf{x} as points in an oriented projective plane \mathbf{T}^2 . Notice that in standard projective geometry, given a projective point \mathbf{x} , $\lambda\mathbf{x}$ represents the same point whenever $\lambda \neq 0$. In an oriented projective plane this is only true if $\lambda > 0$ [17]. This is important when modelling panoramic vision sensors where diametrically opposite points relative to the projection center can be simultaneously imaged.

$$\mathbf{x}_{cam} = \mathbf{M}_c \cdot \mathbf{f}(\mathbf{x}) \quad (1)$$

$$\mathbf{M}_c = \begin{bmatrix} \psi - \xi & 0 & 0 \\ 0 & \xi - \psi & 0 \\ 0 & 0 & 1 \end{bmatrix} \quad (2)$$

$$\mathbf{f}(\mathbf{x}) = \left(\frac{x}{\sqrt{x^2 + y^2 + z^2}}, \frac{y}{\sqrt{x^2 + y^2 + z^2}}, \frac{z}{\sqrt{x^2 + y^2 + z^2}} + \xi \right)^t \quad (3)$$

To each oriented projective ray/point \mathbf{x} , corresponds a projective ray/point \mathbf{x}_{cam} in a coordinate system whose origin is in the camera projection center. Notice that \mathbf{x} and \mathbf{x}_{cam}

Table 1. Column 1: Reflective surfaces for the different cases of central panoramic imaging. Column 2 and 3: Parameters ξ and ψ of the general central catadioptric model

	Mirror Surface	ξ	ψ
Parabolic	$\sqrt{x^2 + y^2 + z^2} = 2p - z$	1	$1 + 2p$
Hyperbolic	$\frac{(z - \frac{d}{2})^2}{(\frac{1}{2}(\sqrt{d^2 + 4p^2} - 2p))^2} - \frac{x^2 + y^2}{p(\sqrt{d^2 + 4p^2} - 2p)} = 1$	$\frac{d}{\sqrt{d^2 + 4p^2}}$	$\frac{d + 2p}{\sqrt{d^2 + 4p^2}}$
Elliptical	$\frac{(z - \frac{d}{2})^2}{(\frac{1}{2}(\sqrt{d^2 + 4p^2} + 2p))^2} + \frac{x^2 + y^2}{p(\sqrt{d^2 + 4p^2} + 2p)} = 1$	$\frac{d}{\sqrt{d^2 + 4p^2}}$	$\frac{d - 2p}{\sqrt{d^2 + 4p^2}}$
Planar	$z = \frac{d}{2}$	0	1

must intersect in the mirror surface (see Fig.1). We can think of this transformation as a non-linear mapping between two oriented projective planes. The relationship between these two points can be written in the form of equation 1 (the proof is available at [22]). The matrix \mathbf{M}_c depends on the mirror parameters (see equation 2). The parameters ξ and ψ are presented in Table.1. Function $\mathbf{f}()$ is given by equation 3. Notice that $\mathbf{f}(\lambda \mathbf{x}) = \lambda \mathbf{x}$ whenever $\lambda > 0$. $\mathbf{f}()$ is a positive homogeneous function and correspondence $\mathbf{x}_c = \mathbf{f}(\mathbf{x})$ can be interpreted as a non-linear mapping between two oriented projective planes.

$\mathbf{x}_i = \mathbf{K}_c \mathbf{R}_c \mathbf{x}_{cam}$ represents the measured point in the catadioptric image plane. The relation between \mathbf{x}_i and \mathbf{x}_{cam} is established by a collineation depending on camera orientation (matrix \mathbf{R}_c) and camera intrinsic parameters (matrix \mathbf{K}_c). In the case of the hyperbolic and elliptical systems, the fixed viewpoint constraint is verified whenever the camera center is coincident with the second focus of the reflective surface. There are no restrictions on the camera orientation and \mathbf{R}_c is a 3×3 rotation matrix specifying the camera pose. The same can be said when using a planar mirror. For the parabolic situation the camera is orthographic with center at infinity. However there is an important restriction, its image plane must be orthogonal to the paraboloid axis. We are going to assume that $\mathbf{R}_c = \mathbf{I}$ for the parabolic mirror situation.

$$\mathbf{x}_i = \mathbf{H}_c \cdot \mathbf{f}(\mathbf{P} \cdot \mathbf{X}_w^h) \quad (4)$$

$$\mathbf{H}_c = \mathbf{K}_c \cdot \mathbf{R}_c \cdot \mathbf{M}_c \quad (5)$$

A scheme of the proposed model for general central projection is presented in Fig. 2. The mapping between points in the world \mathbf{X}_w and projective points in image \mathbf{x}_i is given by equation 4. Points \mathbf{X}_w^h in projective 3D space are transformed in points \mathbf{x} in the oriented projective plane with origin in the effective viewpoint of the catadioptric systems ($\mathbf{x} = \mathbf{P} \cdot \mathbf{X}_w^h$). Points \mathbf{x} are mapped in points \mathbf{x}_c in a second oriented projective plane. The correspondence function $\mathbf{x}_c = \mathbf{f}(\mathbf{x})$ is non-linear. Projective points \mathbf{x}_i in catadioptric image plane are obtained after a collineation \mathbf{H}_c ($\mathbf{x}_i = \mathbf{H}_c \mathbf{x}_c$).

Figure 2 depicts an intuitive “concrete” model for the proposed general central projection mapping. To each visible point in space corresponds an oriented projective ray \mathbf{x} joining the 3D point with the effective projection center \mathbf{O} . The projective ray intersects a unit sphere centered in \mathbf{O} in a unique point \mathbf{Q} . Consider a point \mathbf{O}_c with coordinates

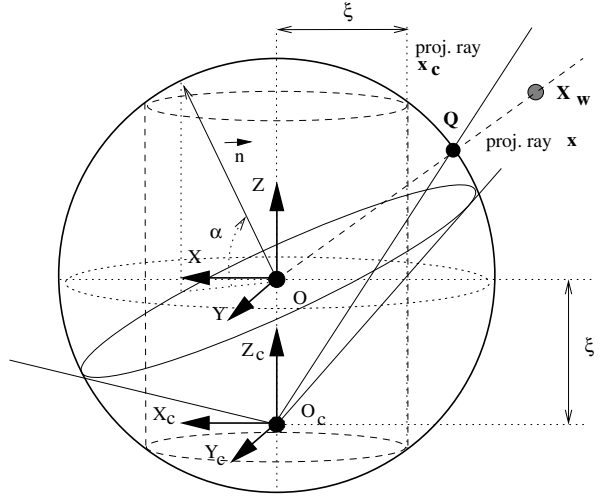
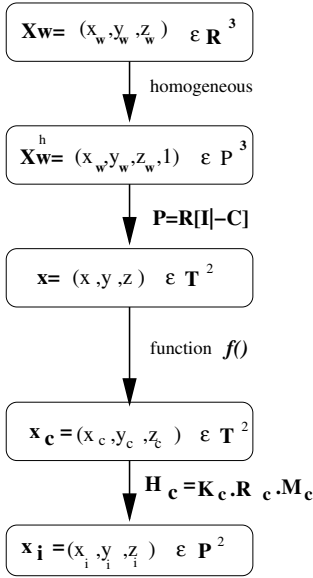


Fig. 2. “Concrete” model for central catadioptric image formation (point and line imaging)

$(0, 0, -\xi)^t$. To each \mathbf{x} corresponds an oriented projective ray \mathbf{x}_c going through O_c and Q . Points in catadioptric image plane x_i (not represented in the figure) are obtained after a collineation H_c of 2D projective points \mathbf{x}_c . The scene is projected in the sphere surface and then points on the sphere are re-projected in catadioptric image plane from a novel projection center O_c . Point O_c only depends on mirror parameters (see Table.1).

3 General Central Catadioptric Imaging of Lines

Assume a line in space lying on plane $\Pi = (n_x, n_y, n_z, 0)^t$ which contains the effective viewpoint O . Accordingly to the model of Fig. 2, line world points X_w are mapped in the oriented projective plane on points \mathbf{x} lying on $\mathbf{n} = (n_x, n_y, n_z)^t$ ($\mathbf{n}^t \cdot \mathbf{x} = 0$).

$$\Omega = \begin{bmatrix} n_x^2(1 - \xi^2) - n_z^2\xi^2 & n_x n_y(1 - \xi^2) & n_x n_z \\ n_x n_y(1 - \xi^2) & n_y^2(1 - \xi^2) - n_z^2\xi^2 & n_y n_z \\ n_x n_z & n_y n_z & n_z^2 \end{bmatrix} \quad (6)$$

The non-linear f mapping (equation 3) establishes the relation between points \mathbf{x} and \mathbf{x}_c . It can be shown that points \mathbf{x} verifying $\mathbf{n}^t \cdot \mathbf{x} = 0$ are mapped into points \mathbf{x}_c which verify $\mathbf{x}_c^t \Omega \mathbf{x}_c = 0$ with Ω given by equation 6). Thus a line in space is mapped into a conic curve Ω . Points \mathbf{x}_c and \mathbf{x}_i in the catadioptric image plane are related by a familiar collineation H_c . Since a projective transformation maps a conic on a conic we can conclude that in general the catadioptric image of a world line is a conic curve. This section assumes $H_c = I$ and the study will focus on the non-linear $f()$ mapping.

Fig.2 depicts central catadioptric line projection using the sphere model. The world line in space is projected into a great circle in the sphere surface. This great circle is the curve of intersection of plane Π , containing both the line and the projection center \mathbf{O} , and the unit sphere. The projective rays \mathbf{x}_c , joining \mathbf{O}_c to points in the great circle, form a central cone surface. The central cone, with vertex in the \mathbf{O}_c , projects into the conic Ω in the canonical image plane. Notice that we can always think of a conic Ω in the projective plane as a central cone of projective rays with vertex in the projection center. Ω is a degenerate conic whenever $n_z = 0$. If the imaged line is co-planar with the Z-axis of the catadioptric reference frame, the corresponding catadioptric image is also a line. This can be easily understood using the sphere model for the mapping.

$$\Delta = (n_x^2 + n_y^2)(1 - \xi^2) - n_z^2\xi \quad (7)$$

$$\alpha = \arctan\left(\frac{n_z}{\sqrt{n_x^2 + n_y^2}}\right) \quad (8)$$

Equation 7 gives the conic discriminant Δ . For $\Delta = 0$, $\Delta > 0$ and $\Delta < 0$ the conic curve Ω is respectively a parabola, an hyperbola and an ellipse/circle. Consider the normal $\mathbf{n} = (n_x, n_y, n_z)^t$ to plane Π (Fig. 2) and the angle α between \mathbf{n} and plane XOY (equation 8). From equation 7 and 8 it results that $\Delta = 0$ whenever $\tan(\alpha)^2 = (1 - \xi^2)/\xi^2$. If the normal to the plane Π intersects the unitary sphere in the dashed circles of Fig. 2 then the line image is a parabola. Moreover if the intersection point is between the circles the line image is an hyperbola and if the intersection point is above or below the circles the line image is an ellipse/circle.

$$\boldsymbol{\mu} = (-n_y, n_x, 0)^t \quad (9)$$

$$\bar{\mathbf{P}}_1, \bar{\mathbf{P}}_2 = \left(-\frac{n_x n_z}{(n_x^2 + n_y^2)(1 \pm \xi \sqrt{1 + \frac{n_z^2}{n_x^2 + n_y^2}})}, -\frac{n_y n_z}{(n_x^2 + n_y^2)(1 \pm \xi \sqrt{1 + \frac{n_z^2}{n_x^2 + n_y^2}})}, 1 \right)^t \quad (10)$$

Affine (center, asymptotes) and euclidean (principal axis, focus, eccentricity) parameters of the conic curve Ω (equation 6) were derived in [12,21] assuming the line at infinity and the circular points at their canonical positions [13,20]. The catadioptric image of a line is the conic curve Ω only if collineation \mathbf{H}_c is the identity. In general $\mathbf{H}_c \neq I$ and the derived affine and euclidean properties do not hold. Equations 9 and 10 present two results that will be needed latter. $\boldsymbol{\mu}$ is one of the principal axis of Ω and $\bar{\mathbf{P}}_1$ and $\bar{\mathbf{P}}_2$ are the points where $\boldsymbol{\mu}$ intersects the conic curve.

4 Geometric Properties of Central Catadioptric Line Images

In the derived central projection model, points in the scene are projected on the surface of an unitary sphere centered in the effective viewpoint \mathbf{O} . The catadioptric image is captured by a conventional perspective camera which projects the points from the sphere

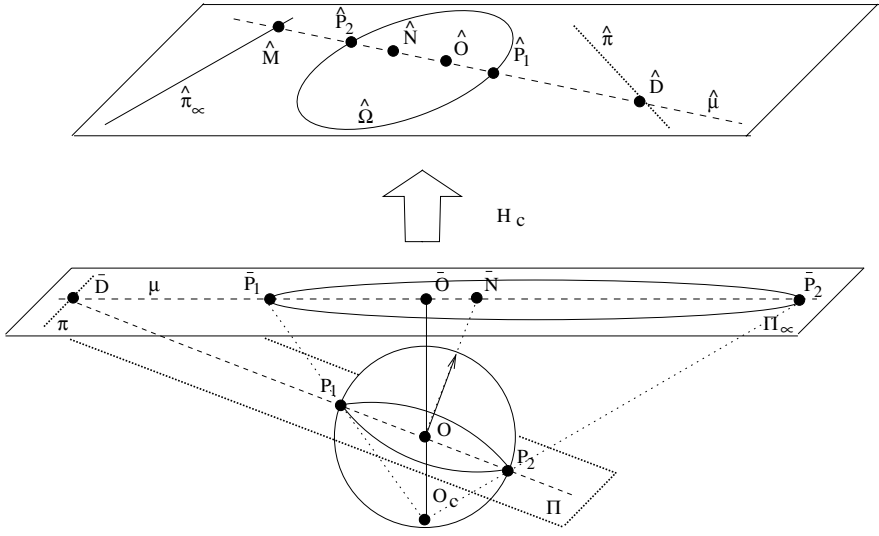


Fig. 3. Projecting sphere points in the plane at infinity and the projective transformation \mathbf{H}_c of Π_∞ in the catadioptric image plane.

to a plane. If $\mathbf{H}_c = \mathbf{I}$ then the image plane is on the canonical position (by canonical we mean orthogonal to the forward looking Z axis). Consider that, whenever $\mathbf{H}_c = \mathbf{I}$, the image plane is the plane at infinity Π_∞ . To each sphere point \mathbf{P} corresponds a projective ray going through the camera center \mathbf{O}_c . Point \mathbf{P} projects on $\bar{\mathbf{P}}$ which is the intersection of the projective ray $\mathbf{O}_c\mathbf{P}$ with Π_∞ .

Consider a line in the scene which lies in plane Π depicted in Fig.3. Π , going through the effective viewpoint \mathbf{O} with normal \mathbf{n} , intersects the spherical surface in a great circle. Points on the great circle define a central cone of projective rays with vertex in \mathbf{O}_c . The central cone of projective rays intersect Π_∞ in the conic curve Ω (equation 6). Moreover a pencil of parallel planes intersects Π_∞ in the same line (the horizon line) and a pencil of parallel lines intersects Π_∞ in the same point (the direction point). Returning to Fig. 3, π is the horizon line of plane Π , $\bar{\mathbf{D}}$ is the direction point of line $\mathbf{P}_1\mathbf{P}_2$, and $\bar{\mathbf{N}}$ is the direction orthogonal to Π . Notice that space line $\mathbf{P}_1\mathbf{P}_2$ lies on plane Π thus $\pi^t\bar{\mathbf{D}} = 0$. Moreover lines $\mathbf{P}_1\mathbf{P}_2$, $\mathbf{O}_c\mathbf{O}$, projective rays $\mathbf{O}_c\mathbf{P}_1$, $\mathbf{O}_c\mathbf{P}_2$ and the normal \mathbf{n} are co-planar, thus the corresponding direction points $\bar{\mathbf{D}}$, $\bar{\mathbf{O}}$, $\bar{\mathbf{P}}_1$, $\bar{\mathbf{P}}_2$ and $\bar{\mathbf{N}}$ are all collinear.

Collineation \mathbf{H}_c depends on camera intrinsic parameters, the relative rotation between the imaging device and the reflective surface, and mirror parameters (equation 5). In general $\mathbf{H}_c \neq \mathbf{I}$ and the catadioptric image and Π_∞ are related by a general projective transformation between planes (Fig. 3). A generic point $\bar{\mathbf{P}}$ is mapped in $\hat{\mathbf{P}} = \mathbf{H}_c\bar{\mathbf{P}}$, the conic curve Ω is imaged in $\hat{\Omega} = \mathbf{H}_c^{-t}\Omega\mathbf{H}_c^{-1}$, and the line μ is transformed in $\hat{\mu} = \mathbf{H}_c^{-t}\mu$ [13,19].

In general the projective transformation \mathbf{H}_c changes the position of the line at infinity and the circular conic envelope Ω_∞ . If $\mathbf{H}_c \neq \mathbf{I}$ the affine and euclidean parameters

derived for the conic curve Ω in [12,21] do not hold. This is illustrated in Fig. 3 for the major axis μ . From equation 9 one concludes that both the principal point $\bar{\mathbf{O}} = (0, 0, 1)^t$ and the direction point of the normal $\bar{\mathbf{N}} = (n_x, n_y, n_z)^t$ lie on μ ($\mu^t \bar{\mathbf{O}} = \mu^t \bar{\mathbf{N}} = 0$). Thus the major axis μ is the intersection line between Π_∞ and the plane containing both the normal direction \mathbf{n} and the Z axis. The collineation \mathbf{H}_c between Π_∞ and the catadioptric image plane maps μ in $\hat{\mu}$ and Ω in $\hat{\Omega}$. In general $\hat{\mu}$ is no longer a principal axis of $\hat{\Omega}$. Nevertheless the projective transformation preserves collinearity, incidence and the cross-ratio. These invariants will be exploited to establish geometric relations for line catadioptric imaging when $\mathbf{H}_c \neq \mathbf{I}$.

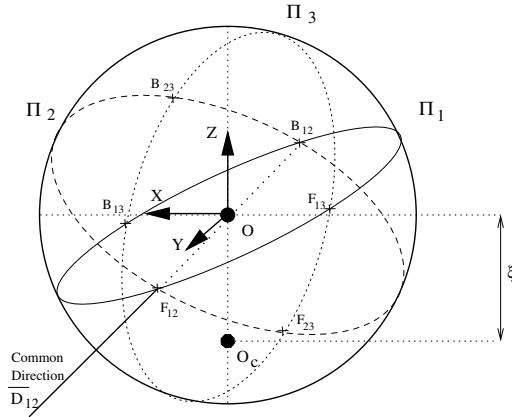


Fig. 4. Three world lines projected on the unitary sphere.

4.1 Three Catadioptric Line Images

Consider three world lines visible in the catadioptric image plane. Configurations leading to degenerate conics Ω are excluded. Thus the imaged lines are not co-planar with the Z axis and the central catadioptric system is not a perspective camera.

The three world lines lie on planes Π_1 , Π_2 and Π_3 , with normals \mathbf{n}_1 , \mathbf{n}_2 and \mathbf{n}_3 , going through the effective viewpoint \mathbf{O} . As depicted in Fig. 4, each plane intersects the unit sphere in a great circle. Great circles lying in planes Π_i and Π_j intersect in antipodal points \mathbf{F}_{ij} and \mathbf{B}_{ij} . Line $\mathbf{F}_{ij}\mathbf{B}_{ij}$, containing the effective viewpoint \mathbf{O} , intersects the plane at infinity Π_∞ in point $\bar{\mathbf{D}}_{ij}$. $\bar{\mathbf{D}}_{ij}$ is the common direction of planes Π_i and Π_j . Moreover planes Π_1 , Π_2 and Π_3 intersect Π_∞ in lines π_1 , π_2 and π_3 (the horizon lines), and the direction points of normal vectors \mathbf{n}_1 , \mathbf{n}_2 and \mathbf{n}_3 are $\bar{\mathbf{N}}_1$, $\bar{\mathbf{N}}_2$ and $\bar{\mathbf{N}}_3$.

4.2 The Principal Point $\hat{\mathbf{O}}$ and the Absolute Conic $\hat{\Omega}_\infty$ in the Catadioptric Image Plane

The three world lines are projected in the catadioptric image plane in conic curves $\hat{\Omega}_1$, $\hat{\Omega}_2$ and $\hat{\Omega}_3$ as depicted in Fig. 5. In general two conic curves intersect in four points [16].

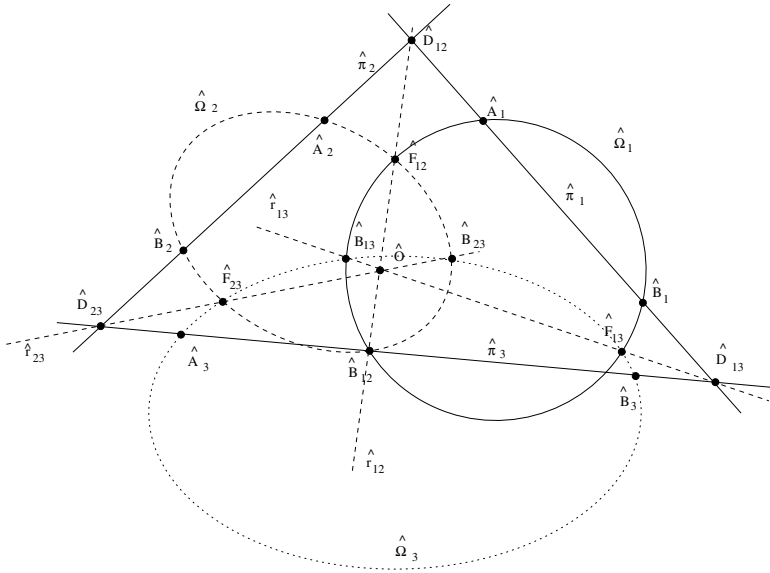


Fig. 5. Determining the principal point and the absolute conic from three catadioptric line images

If the camera, with center in point O_c , is forward looking then only two real intersection points are visible in the catadioptric image (Fig. 4). Any pair of conic curves $\hat{\Omega}_i$ and $\hat{\Omega}_j$, intersect on \hat{F}_{ij} and \hat{B}_{ij} which are the catadioptric image of the antipodal points F_{ij} and B_{ij} . Line \hat{r}_{ij} goes through the two intersection points of conic curves $\hat{\Omega}_i$ and $\hat{\Omega}_j$ ($\hat{r}_{ij} = \hat{F}_{ij} \wedge \hat{B}_{ij}$).

Proposition 1: Consider the line catadioptric images $\hat{\Omega}_i$ and $\hat{\Omega}_j$ intersecting on \hat{F}_{ij} and \hat{B}_{ij} . The catadioptric image center \hat{O} is always collinear with the intersection points of the two conics.

Proof: The effective viewpoint O always lies in the plane defined by the two antipodal points F_{ij} , B_{ij} and the camera center O_c (Fig. 4). Consider the intersection line r_{ij} of plane $O_c F_{ij} B_{ij}$ with Π_∞ . Since plane $O_c F_{ij} B_{ij}$ contains projective rays $O_c F_{ij}$, $O_c B_{ij}$ and $O_c O$, then points \bar{F}_{ij} , \bar{B}_{ij} and \bar{O} must lie in r_{ij} . The projective transformation H_c preserves collinearity, thus \hat{O} must lie on \hat{r}_{ij} .

Corollary 1: The image center \hat{O} can be determined from three catadioptric line images $\hat{\Omega}_1$, $\hat{\Omega}_2$ and $\hat{\Omega}_3$ whenever the lines \hat{r}_{12} , \hat{r}_{13} and \hat{r}_{23} are not coincident.

Lines \hat{r}_{12} , \hat{r}_{13} and \hat{r}_{23} are coincident whenever the three world lines project on three great circles in the sphere surface which intersect in the same pair of antipodal points (see Fig. 4). This exception only occurs if the rank of matrix $[II_1 II_2 II_3]$ is less than 3

which means that the three imaged world lines can be intersected by a same line going through the effective viewpoint \mathbf{O} .

Proposition 2: *The conic of points $\hat{\Omega}$ is the catadioptric image of a line in space lying on a plane Π going through the effective viewpoint. The intersection line π of Π with Π_∞ is mapped on $\hat{\pi}$ in the catadioptric image plane, which is the polar line of the image center $\hat{\mathbf{O}}$ with respect to conic locus $\hat{\Omega}$ ($\hat{\pi} = \hat{\Omega}.\hat{\mathbf{O}}$).*

Proof: The plane Π , containing the imaged line, intersects the unitary sphere in a great circle. Consider a generic line, lying on Π and going through the effective viewpoint \mathbf{O} , with direction point $\bar{\mathbf{D}}$ (Fig. 3). The line intersects the great circle in two antipodal points \mathbf{P}_1 and \mathbf{P}_2 which are equidistant to \mathbf{O} . This implies that, in the plane at infinity, points $\bar{\mathbf{D}}$ and $\bar{\mathbf{O}}$ are harmonic with respect to $\bar{\mathbf{P}}_1$ and $\bar{\mathbf{P}}_2$. Points $\bar{\mathbf{P}}_1$ and $\bar{\mathbf{P}}_2$ lie in the conic curve Ω , and the locus of direction points $\bar{\mathbf{D}}$ is the horizon line π of plane Π . Thus π is the polar of $\bar{\mathbf{O}}$ with respect to Ω . The catadioptric image is related with the plane at infinity by a collineation \mathbf{H}_c . The proposition is proved since pole/polar relations are invariant under a projective transformation.

Corollary 2: *Consider two lines lying on planes Π_i and Π_j , imaged in the conic curves $\hat{\Omega}_i$ and $\hat{\Omega}_j$. The common direction $\bar{\mathbf{D}}_{ij}$ of the two planes is mapped in the catadioptric image at $\hat{\mathbf{D}}_{ij}$, which is the intersection point of lines $\hat{\pi}_i$, $\hat{\pi}_j$ and $\hat{\mathbf{r}}_{ij}$. Moreover, if the two imaged lines are parallel, then they intersect Π_∞ at point $\bar{\mathbf{D}}$ which is mapped at $\hat{\mathbf{D}} = \hat{\mathbf{D}}_{ij}$.*

Planes Π_i and Π_j intersect on line $\mathbf{F}_{ij}\mathbf{B}_{ij}$ with direction $\bar{\mathbf{D}}_{ij}$ as depicted in Fig. 4. Since the direction is common to both planes then $\bar{\mathbf{D}}_{ij}$ lies on both vanishing lines π_i and π_j . Moreover plane $\mathbf{F}_{ij}\mathbf{O}_c\mathbf{B}_{ij}$, containing the line $\mathbf{F}_{ij}\mathbf{B}_{ij}$, intersect Π_∞ on \mathbf{r}_{ij} which goes through $\bar{\mathbf{D}}_{ij}$. The projective transformation \mathbf{H}_c preserves incidence thus $\hat{\mathbf{D}}_{ij}$ lies on the three lines $\hat{\pi}_i$, $\hat{\pi}_j$ and $\hat{\mathbf{r}}_{ij}$. If the imaged world lines are parallel then the common direction of planes Π_i and Π_j is the line direction $\bar{\mathbf{D}}$.

Knowing collineation \mathbf{H}_c and the image center $\hat{\mathbf{O}}$, it is possible to recover the orientation of any world plane Π from the catadioptric image of two sets of parallel lines lying on it. Assume that one set intersects in the plane at infinity at $\bar{\mathbf{D}}$, and the other at $\bar{\mathbf{D}}'$. The direction points are mapped in the catadioptric image plane at points $\hat{\mathbf{D}}$ and $\hat{\mathbf{D}}'$ which can be determined from the results of proposition 2 and corollary 2. Since both $\bar{\mathbf{D}}$ and $\bar{\mathbf{D}}'$ must lie on the horizon line of plane Π it comes that π is mapped on $\hat{\pi} = \hat{\mathbf{D}} \wedge \hat{\mathbf{D}}'$. If \mathbf{H}_c is known then the horizon line of Π is $\pi = \mathbf{H}_c^t \hat{\pi}$ and the orientation of the plane can be recovered.

Proposition 3: *Consider that the absolute conic Ω_∞ is mapped on conic $\hat{\Omega}_\infty$ at the catadioptric image plane. If $\hat{\Omega}$ is the catadioptric image of a line in space, then the polar line $\hat{\pi}$ of the image center $\hat{\mathbf{O}}$ ($\hat{\pi} = \hat{\Omega}.\hat{\mathbf{O}}$) intersects the conic locus $\hat{\Omega}$ in two points $\hat{\mathbf{A}}$ and $\hat{\mathbf{B}}$ which belong to $\hat{\Omega}_\infty$.*

Proof: In general a quadric in space intersects a plane in a conic curve. Assume Ω as the

intersection of a quadric \mathbf{Q} with the plane at infinity Π_∞ . Two conics curves intersect in four points. Consider the points of intersection of Ω with the absolute conic Ω_∞ . Each pair of intersection points $\bar{\mathbf{A}}$ and $\bar{\mathbf{B}}$ defines a line which is the horizon line of a pencil of parallel planes (real or complex). Moreover each plane in the pencil intersects the original quadric \mathbf{Q} in a conic going through points $\bar{\mathbf{A}}$ and $\bar{\mathbf{B}}$. Since $\bar{\mathbf{A}}$ and $\bar{\mathbf{B}}$ are the circular points of the plane one concludes that the intersection conic is a circle. Thus the pencil of parallel planes intersect the quadric in circular sections [15]. Fig. 3 shows that a line in space projects in a great circle in the sphere surface. The great circle defines a central cone \mathbf{Q} of projective rays with vertex in \mathbf{O}_c , which intersects Π_∞ in Ω . According to proposition 2, $\pi = \Omega \cdot \bar{\mathbf{O}}$ is the horizon line of the plane Π , going through the effective viewpoint, and containing the imaged line. The plane cuts the central cone \mathbf{Q} of projective rays in a circular section (the great circle). Thus the corresponding horizon line π intersects Ω in two circular points which lie in the absolute conic Ω_∞ . The established relations hold in the catadioptric image plane after the projective transformation \mathbf{H}_c .

Corollary 3: *The absolute conic $\hat{\Omega}_\infty$ in the catadioptric image plane can be determined from the three image lines $\hat{\Omega}_1$, $\hat{\Omega}_2$ and $\hat{\Omega}_3$*

For each conic locus compute the polar line of the image center $\hat{\mathbf{O}}$ and determine the two intersection points of the obtained line with the original conic curve. Six points of $\hat{\Omega}_\infty$ are obtained: $\hat{\mathbf{A}}_1, \hat{\mathbf{B}}_1, \hat{\mathbf{A}}_2, \hat{\mathbf{B}}_2, \hat{\mathbf{A}}_3$ and $\hat{\mathbf{B}}_3$ (see Fig. 5). Since five points define a conic locus, the six points are sufficient to estimate $\hat{\Omega}_\infty$.

4.3 Estimating Mirror Parameters from the Catadioptric Projection of Lines

Assume that both the catadioptric image center $\hat{\mathbf{O}}$ and the absolute conic $\hat{\Omega}_\infty$ are known. The conic curve $\hat{\Omega}$ is the catadioptric image of a line in space lying on plane Π going through the center \mathbf{O} of the catadioptric system. From proposition 2 it results that $\hat{\pi} = \hat{\Omega} \cdot \hat{\mathbf{O}}$ is the locus where the horizon line of Π is mapped. If $\bar{\mathbf{N}}$ is the direction point of the normal to the plane then $\bar{\mathbf{N}}$ is mapped on $\hat{\mathbf{N}} = \hat{\Omega}_\infty \cdot \bar{\mathbf{N}}$ at the catadioptric image plane.

Proposition 4: *Consider the normal direction $\bar{\mathbf{N}}$ of a plane Π containing the effective viewpoint. If $\bar{\mathbf{N}}$ is mapped on $\hat{\mathbf{N}}$ then the major axis μ of the projection Ω on Π_∞ of a line lying on Π is mapped on $\hat{\mu} = \hat{\mathbf{O}} \wedge \hat{\mathbf{N}}$*

Proof: Figure3 depicts the major axis μ as the intersection of plane at infinity with the plane defined by the normal vector \mathbf{n} to Π and the Z axis. This result comes directly from equation 9. Notice that both $\bar{\mathbf{O}}$ and $\bar{\mathbf{N}}$ lie on μ . Since collineation \mathbf{H}_c preserves incidence comes that both points $\hat{\mathbf{O}}$ and $\hat{\mathbf{N}}$ must lie on the locus $\hat{\mu}$ where μ is mapped.

Corollary 4: *If the conic of points $\hat{\Omega}$ is the catadioptric image of a line lying on Π then the pole of $\hat{\mu}$ with respect to $\hat{\Omega}$ lies on $\hat{\pi}_\infty$ which is the intersection line of the catadioptric image plane with the plane at infinity Π_∞ .*

Corollary 5: *If both the catadioptric image center $\hat{\mathbf{O}}$ and absolute conic $\hat{\Omega}_\infty$ are known, it is possible to determine the position of the line at infinity $\hat{\pi}_\infty$ from two distinct catadioptric line images.*

The major axis μ is a diameter of the conic Ω , thus the corresponding pole lies in the line at infinity π_∞ [20]. Since the pole/polar relations are preserved under a projective transformation comes that point $\hat{\Omega}^* \hat{\mu}$ must lie on $\hat{\pi}_\infty$ ($\hat{\Omega}^*$ is the conic envelope of $\hat{\Omega}$). Corollary 5 arises from the fact that a line is defined by two points. Notice that if $\hat{\pi}_\infty$ is on the canonical position $(0, 0, 1)^t$ then \mathbf{H}_c is an affine transformation and the camera is not rotated with respect to the reflective surface ($\mathbf{R} = \mathbf{I}$ in equation 5). Points $\hat{\mathbf{D}}$ and $\hat{\mathbf{M}}$, depicted on Fig. 3, are the intersection points of $\hat{\mu}$ with the horizon line of Π and the line at infinity at the catadioptric image plane ($\hat{\mathbf{D}} = \hat{\mu} \wedge \hat{\pi}$ and $\hat{\mathbf{M}} = \hat{\mu} \wedge \hat{\pi}_\infty$).

Proposition 5: *The cross ratio of points $\hat{\mathbf{O}}$, $\hat{\mathbf{M}}$, $\hat{\mathbf{D}}$ and $\hat{\mathbf{N}}$ lying on $\hat{\mu}$, only depends on the angle between plane Π and plane XOY of the catadioptric reference frame. In particular $\{\hat{\mathbf{D}}, \hat{\mathbf{N}}; \hat{\mathbf{O}}, \hat{\mathbf{M}}\} = -\tan(\alpha)^2$ with α the angle of equation 8.*

Proof: Consider the major axis μ depicted on Fig. 3 given in equation 9. The origin of Π_∞ is $\bar{\mathbf{O}} = (0, 0, 1)^t$ and the normal vector \mathbf{n} intersects the plane at infinity at $\bar{\mathbf{N}} = (n_x, n_y, n_z)^t$. Moreover the intersection point $\bar{\mathbf{D}}$ of μ and π is $\bar{\mathbf{D}} = \mu \wedge \pi = (-n_x n_z, -n_y n_z, n_x^2 + n_y^2)^t$. Point $\hat{\mathbf{M}}$ is the direction point of μ . The line at infinity π_∞ is on the canonical position thus, from equation 9, results $\hat{\mathbf{M}} = (n_x, n_y, 0)^t$. Computing the cross-ratio between the four points arises $\{\bar{\mathbf{D}}, \bar{\mathbf{N}}; \bar{\mathbf{O}}, \bar{\mathbf{M}}\} = -\tan(\alpha)^2$. The cross-ratio is a projective invariant and the proposition is proved.

Proposition 6: *Consider point $\hat{\mathbf{P}}_1$ and $\hat{\mathbf{P}}_2$ where line $\hat{\mu}$ intersects the corresponding conic locus $\hat{\Omega}$ (the catadioptric line image). The cross ratio of points $\hat{\mathbf{D}}$, $\hat{\mathbf{N}}$, $\hat{\mathbf{P}}_1$ and $\hat{\mathbf{P}}_2$ depends on catadioptric system parameter ξ and on angle α (equation 8). In particular $2\{\hat{\mathbf{P}}_1, \hat{\mathbf{D}}; \hat{\mathbf{N}}, \hat{\mathbf{P}}_2\} = 1 + \xi |\cot(\alpha)|$.*

Proof: At the plane at infinity Π_∞ , major axis μ intersects conic locus Ω on points $\bar{\mathbf{P}}_1$ and $\bar{\mathbf{P}}_2$ provided by equation 10 (see Fig. 3). Computing the cross-ratio it comes $\{\bar{\mathbf{P}}_1, \bar{\mathbf{D}}; \bar{\mathbf{N}}, \bar{\mathbf{P}}_2\} = \frac{1 + \xi |\cot(\alpha)|}{2}$. Points $\bar{\mathbf{P}}_1$, $\bar{\mathbf{P}}_2$, $\bar{\mathbf{D}}$ and $\bar{\mathbf{N}}$ mapped on the catadioptric image plane at points $\hat{\mathbf{P}}_1$, $\hat{\mathbf{P}}_2$, $\hat{\mathbf{D}}$ and $\hat{\mathbf{N}}$ by collineation \mathbf{H}_c which preserves the cross-ratio.

Corollary 6: *Consider the points $\hat{\mathbf{O}}$, $\hat{\mathbf{N}}$, $\hat{\mathbf{D}}$, $\hat{\mathbf{M}}$, $\hat{\mathbf{P}}_1$ and $\hat{\mathbf{P}}_2$ lying on line $\hat{\mu}$ associated with catadioptric line image $\hat{\Omega}$, as depicted in Fig. 3. The ξ parameter of the central catadioptric system is $\xi = (2\{\hat{\mathbf{P}}_1, \hat{\mathbf{D}}; \hat{\mathbf{N}}, \hat{\mathbf{P}}_2\} - 1) \sqrt{-\{\hat{\mathbf{D}}, \hat{\mathbf{N}}; \hat{\mathbf{O}}, \hat{\mathbf{M}}\}}$*

5 Calibration Algorithm and Results

The previous section shows that it is possible to estimate the catadioptric image center and the absolute conic from three line images. Moreover it is possible to estimate the

position of the line at infinity and the ξ parameter of the catadioptric vision system. In this section we use the established propositions to derive the following calibration algorithm.

1. *Identify in the catadioptric image three distinct non-degenerate line images (each line must project on a proper conic)*
2. *Fit the three conics $\hat{\Omega}_1$, $\hat{\Omega}_2$ and $\hat{\Omega}_3$ [23].*
3. *For each pair of conics $\hat{\Omega}_i$ and $\hat{\Omega}_j$, determine the intersection points $\hat{\mathbf{F}}_{ij}$ and $\hat{\mathbf{B}}_{ij}$ and compute line $\hat{\mathbf{r}}_{ij} = \hat{\mathbf{F}}_{ij} \wedge \hat{\mathbf{B}}_{ij}$.*
4. *Estimate the image center $\hat{\mathbf{O}}$ as the intersection point of lines $\hat{\mathbf{r}}_{12}$, $\hat{\mathbf{r}}_{13}$ and $\hat{\mathbf{r}}_{23}$.*
5. *For each conic $\hat{\Omega}_i$ compute the polar $\hat{\pi}_i$ of image center $\hat{\mathbf{O}}$.*
6. *Obtain points $\hat{\mathbf{A}}_1$, $\hat{\mathbf{B}}_1$, $\hat{\mathbf{A}}_2$, $\hat{\mathbf{B}}_2$, $\hat{\mathbf{A}}_3$ and $\hat{\mathbf{B}}_3$ by intersecting $\hat{\pi}_1$, $\hat{\Omega}_1$; $\hat{\pi}_2$, $\hat{\Omega}_2$ and $\hat{\pi}_3$, $\hat{\Omega}_3$.*
7. *Fit the conic going through the 6 points $\hat{\mathbf{A}}_1$, $\hat{\mathbf{B}}_1$, $\hat{\mathbf{A}}_2$, $\hat{\mathbf{B}}_2$, $\hat{\mathbf{A}}_3$ and $\hat{\mathbf{B}}_3$. The result $\hat{\Omega}_\infty$ is the absolute conic at the catadioptric image plane.*
8. *For each line $\hat{\pi}_i$ compute the pole $\hat{\mathbf{N}}_i$ with respect to the estimated absolute conic ($\hat{\mathbf{N}}_i = \hat{\Omega}_\infty^* \cdot \hat{\pi}_i$ for $i = 1, 2, 3$).*
9. *Obtain the line $\hat{\mu}_i$ going through point $\hat{\mathbf{N}}_i$ and the image center $\hat{\mathbf{O}}$ ($\hat{\mu}_i = \hat{\mathbf{O}} \wedge \hat{\mathbf{N}}_i$ for $i = 1, 2, 3$).*
10. *Estimate the line at infinity $\hat{\pi}_\infty$ as the line going through the poles $\hat{\Omega}_i^* \cdot \hat{\mu}_i$.*
11. *For each line $\hat{\mu}_i$, obtain the intersection points $\hat{\mathbf{D}}_i$, $\hat{\mathbf{M}}_i$ with lines $\hat{\pi}_i$ and $\hat{\pi}_\infty$ ($\hat{\mathbf{D}}_i = \hat{\mu}_i \wedge \hat{\pi}_i$ and $\hat{\mathbf{D}}_i = \hat{\mu}_i \wedge \hat{\pi}_\infty$) and $\hat{\mathbf{P}}_{1i}$, $\hat{\mathbf{P}}_{2i}$ with conic $\hat{\Omega}_i$.*
12. *Estimate parameter ξ averaging the estimations $\xi_i = (2\{\hat{\mathbf{P}}_{1i}, \hat{\mathbf{D}}_i; \hat{\mathbf{N}}_i, \hat{\mathbf{P}}_{2i}\} - 1)\sqrt{-\{\hat{\mathbf{D}}_i, \hat{\mathbf{N}}_i; \hat{\mathbf{O}}_i, \hat{\mathbf{M}}_i\}}$ for $i = 1, 2, 3$.*

The principal point can be directly extracted from the estimation of $\hat{\mathbf{O}}$. From the position of the line at infinity it is possible to determine if the camera is rotated with respect to the reflective surface. If $\hat{\pi}_\infty$ is on the canonical position then \mathbf{H}_c is an affine transformation. Thus, from equation 5, the rotation matrix \mathbf{R} is equal to the identity and $\mathbf{H}_c = \mathbf{K}_c \mathbf{M}_c$. In this case \mathbf{H}_c is upper triangular and it can be determined from $\hat{\Omega}_\infty$ using Cholesky factorization [13]. If $\hat{\pi}_\infty$ is not in the canonical position, then $\mathbf{R} \neq \mathbf{I}$ and \mathbf{H}_c must be estimated using stratified methods.

This algorithm has been validated by simulation. In practical application the performance of the algorithm highly depends on the accuracy of the conic fitting method.

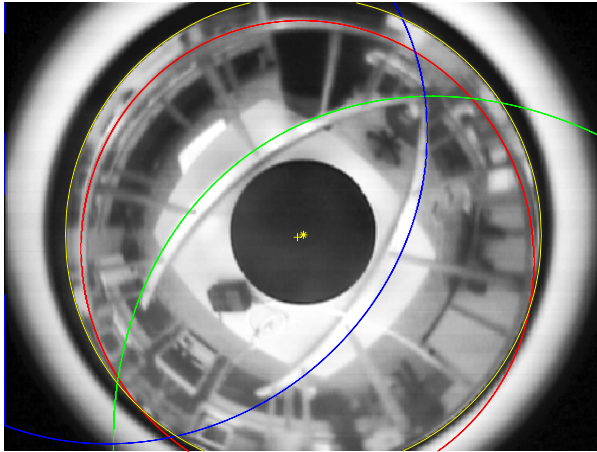


Fig. 6. The calibration algorithm. The green, red and blue lines are the fitted catadioptric line images $\hat{\Omega}_1$, $\hat{\Omega}_2$ and $\hat{\Omega}_3$. The mirror boundary is under the yellow line. The image center using our algorithm (+) and the mirror boundary algorithm (*)

Some experiments have been made using parabolic images (Fig. 6). Total least square estimation using SVD decomposition have been used for both conic fitting and point/line estimation. Without a specific conic fitting algorithm we have correctly estimated the line at infinity at the canonical position and an unitary parameter ξ .

6 Conclusions

In this paper several new results that apply to central catadioptric images were derived. All the results obtained are based on the images of lines. In addition the theoretical results presented show how the orientation of a plane in space can be computed for the all class of catadioptric systems. With the knowledge of the absolute conic it is also possible to find out when two lines are perpendicular.

References

1. T. Svoboda, T. Pajdla and V. Hlavac, "Motion Estimation Using Central Panoramic Cameras," *Proc. IEEE Conference on Intelligent Vehicles, Stuttgart Germany 1998*.
2. J. Gluckman and S. Nayar, "Egomotion and Omnidirectional Cameras," *ICCV98 - Proc. IEEE International Conference on Computer Vision*, pp. 999-1005, Bombay 1998.
3. E. Hecht and A. Zajac, *Optics*, Addison-Wesley, 1974
4. E. Malis, F. Chaumette, and S. Boudet, "2 1/2 d visual servoing," *IEEE Trans. on Robotics and Automation*, vol. 15, no. 2, pp. 238-250, April 1999.
5. S. Bogner, "Introduction to panoramic imaging," in *Proc. of IEEE SMC Conference*, October 1995, pp. 3100 - 3106.
6. V. S. Nalwa, "A true omnidirectional viewer," *Technical Report, Bell Laboratories*, Holmdel, NJ, USA, February 1996.

7. Y. Yagi and S. Kawato, "Panoramic scene analysis with conic projection," in *Proc. of the International Conference on Robots and Systems*, 1990.
8. K. Yamazawa, Y. Yagi, and M. Yachida, "Omnidirectional imaging with hyperboloidal projection," in *Proc. of the International Conference on Robots and Systems*, 1993.
9. K. Yamazawa, Y. Yagi, and M. Yachida, "Obstacle avoidance with omnidirectional image sensor hyperomni vision," in *Proc. of the IEEE International Conference on Robotics and Automation*, May 1995, pp. 1062 – 1067.
10. S. Baker and S. Nayar, "A Theory of Catadioptric Image Formation," *ICCV98 - Proc. IEEE International Conference on Computer Vision*, pp. 35-42, Bombay 1998.
11. T. Svoboda, T. Pajdla and V. Hlavac, "Epipolar Geometry for Panoramic Cameras," *ECCV98-Proc. Of 5th European Conference on Computer Vision*, pp 218-332, Freiburg Germany 1998.
12. C. Geyer and K. Daniilidis, "A Unifying Theory for Central Panoramic Systems and Pratical Implications," *ECCV2000-Proc. European Conference on Computer Vision*, pp. 445-461, Dublin 2000.
13. R. Hartley and A. Zisserman, '*Multiple View geometry in Computer Vision*, Cambridge University Press, 2000.
14. C. Geyer and K. Daniilidis, "Catadioptric Camera Calibration", *ICCV99 - Proc. of IEEE International Conference on Computer Vision*, pp. 398-403, Corfu, Greece, 1999.
15. Barry Spain, *Analytical Quadrics*, Pergamon Press, 1960.
16. Barry Spain, *Analytical Conics*, Pergamon Press, 1957.
17. S. Laveau and O. Faugeras, "Oriented Projective Geometry for Computer Vision", *ECCV96 - Proc. of European Conference on Computer Vision*, 1996
18. Jorge Stolfi, *Oriented Projective Geometry*, Academic Press Inc., 1991.
19. O. Faugeras, *Three-dimensional computer vision, a Geometric Viewpoint*, MIT Press, 1993.
20. J. G. Semple, G. T. Kneebone, *Algebraic Projective Geometry*, Clarendon Press, 1998.
21. Joao P. Barreto and H. Araujo, "Issues on the geometry of central catadioptric imaging," in *Proc. of the IEEE Int. Conf. on Computer Vision and Pattern Recognition*, Kauai, Haway, USA, December 2001.
22. Joao P. Barreto and H. Araujo, "Study of the Geometry of Central Catadioptric Systems," *ISR Technical Report*, Coimbra, May 2001.
23. Z. Zhang, *Parameter Estimation Techniques: A Tutorial with Application to Conic Fitting*, INRIA Raport de Recherche n 2676, October 1995.